2009 IEEE/ASME International Conference on Advanced Intelligent Mechatronics
Suntec Convention and Exhibition Center
Singapore, July 14-17, 2009

A Novel Temperature based Flat-Plate Heat Flux Sensor for High Accuracy Measurement

Dongxiao Liu, Yun-Ze Li, *IEEE Member*, Yunhua Li, *IEEE Member*,
and Kok-Meng Lee, *IEEE/ASME Fellow*

***Abstract*—This paper presents a novel flat-plate heat-flux sensor for thermal control systems of airborne electronic equipments and actuators. The sensor consists of a pair of high and low conductivity materials to enable the temperature difference between the heat source and heat sink to be measured by resistance temperature detectors (RTDs) and an auxiliary conditioning circuit. Because high accuracy RTDs are installed on the surfaces of the temperature component and the heat flux can be accurately calculated according to the Fourier conduction law, this sensor can acquire high-accuracy measurements. Specifically, this paper details the operating principle and design of a heat flux sensor, discusses methods for improving the heat flux resolution, presents a computational algorithm (with experimentally validation) for a prototype sensor, and demonstrates the application of a flat-plate heat-flux sensor as an equivalent physical simulator (EPS) for a nano-satellite. Two design configurations are experimentally compared providing intuitive insights to the effects of the key parameters on the sensor performance. Experimental studies show that the flat- plate heat-flux sensor has a sensitivity in the order of 0.001-0.01K/(W/m^2).**

***Index terms*—temperature difference, heat flux, measurement accuracy, data processing**

I. Introduction

Measurement of the heat flux (or the quantity of thermal energy transferring through per unit area) is important for the heat transfer and thermal control of airborne equipments (including intelligent instruments, actuators, line replacement units). Because the heat flux is proportional to the temperature gradient, it can provide more predicted information than that deduced from temperature. Accordingly, taking heat flux as a feedback variable in thermal control system can acquire better effects.

Thermal management has been researched widely, especially on electronic devices [1,2] and spacecraft [3,4], where temperature control is a basic and core problem. With the development of dynamic thermal management (DTM), higher requirements for accuracy of temperature control and the level of response speed have been put forward. As feedback variable, heat flux provides a feasible method to improve temperature control accuracy and response speed [5]. Consequently, heat flux measurement is important for implementation of a thermal control system. The measurement method of the heat flux can be classified into three categories: gradient method, transient method, and active heating. The gradient method is the most frequently used principle in heat flux sensor [6]. In previous study, electromotive force (EMF) measurement method based on the Seebeck effect of different metal junctions was researched a lot. Because of high sensitivity on the temperature difference, the method is suitable for the measurement of the convection heat flux, and the kinds of sensors studied include thin film thermocouple heat flux sensor [7], Epoxy- Protected Thermopile heat flux sensor [8], and Bi_x-Sb_x-films heat flux sensor [9]. With the development of semiconductor and microelectronic technology, a new kind of heat flux sensor based on sensitive elements on chip was developed in [10]; its cost is, however, too high for many practical applications. Though these methods embody accession of direct temperature difference signal and quick response to heat flux changes, temperature information cannot be acquired.

Because of several drawbacks in the EMF-based measurement methods, this paper proposes an alternative method for measuring heat flux using RTD (Resistance Temperature Detector). The flat-plate heat-flux sensor presented here employs high-accuracy thin-film RTDs as sensitive elements and high-resolution ADC as signal acquisition element to obtain temperature signals; the new method provides a means to measure heat flux with high accuracy.

The remainder of this paper is organized as follows. Section II describes the operating principle of the flat-plate heat-flux senor. Two improved sensor configurations are implemented, and a measurement circuit is designed. Along with a detailed sensor design, algorithm verification and experimental evaluation of the sensor effectiveness on a specific test bed are described in Section III. Section IV introduces an application where the flat-plate sensor is employed in an equivalent physical simulator for a nano-satellite space radiator. Finally, the conclusions are given in Section V.

This work was supported in part by the National Natural Science Foundation of China under Grant 50506003, by Aeronautic Science Foundation of China under Grant 2008ZC51028 and by Program for Lantian-xinxing Excellent Talents in Beihang University under Grant 2007221237.

Dongxiao Liu and Yunhua Li are with the School of Automation Science and Electrical Engineering, Beihang University, Beijing 100191, China (e-mail: lyz.buaa@gmail.com; yhli@buaa.edu.cn).

Yunze Li is with the School of Aeronautical Science and Engineering, Beihang University, Beijing 100191, China (e-mail: YunzeLi@buaa.edu.cn.

Kok-Meng Lee is with The George W. Woodruff School of Mechanical Engineering, Georgia Institute of Technology, Atlanta, GA 30332-0405, USA(e-mail: kokmeng.lee@me.gatech.edu).

II. Design Concept and Operational Principles

Figure 1 illustrates the operating principle of the flat-plate heat-flux sensor, where the notations are defined in Table I. The heat flux transfers from the heat source through the heat flux sensor (sandwiched between two conductive walls) to the heat sink. The basic sensor configuration consists of a high conductivity thin metal plate, a low conductivity material cylinder, and sensitive elements with two thin-film-resistance temperature detectors (RTDs).

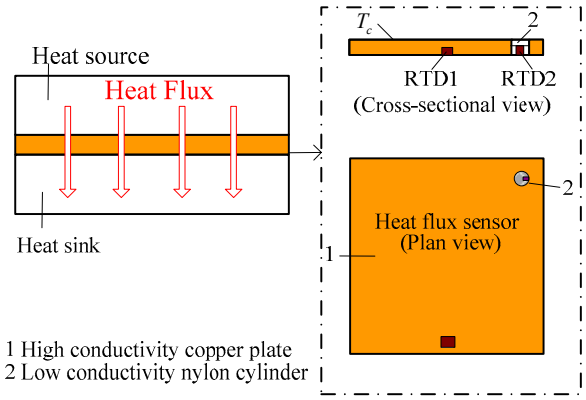

Fig. 1. Operating principle of flat-plate heat-flux sensor

TABLE I
SYMBOL NOTATIONS OF THE SENSOR

T_c	Interface temperature between two different materials
T_1, T_2, T_3	Temperatures of RTD1, RTD2 and RTD3 respectively
q_h, q_l	Heat fluxes through materials 1 and 2 respectively
λ_h, λ_l	Thermal conductivity of materials 1 and 2 respectively
δ_h, δ_l	Thicknesses of materials 1 and 2 respectively

The heat fluxes transfer through the high conductive metal plate and the low conductive material cylinder can be respectively described by (1) and (2) according to Fourier heat conduction law:

$$q_h = -(\lambda_h / \delta_h)\cdot(T_c - T_1) \quad (1)$$

$$q_l = -(\lambda_l / \delta_l)\cdot(T_c - T_2) \quad (2)$$

where the symbols are defined in Table I. Since heat flux density $q=q_h=q_l$, the temperature difference between T_1 and T_2 can be obtained from (1) and (2) by eliminating T_c as follows:

$$\Delta T_{12} = T_1 - T_2 = -q\frac{\delta}{\lambda} \quad \text{where} \quad \frac{\delta}{\lambda} = \frac{\delta_l}{\lambda_l} - \frac{\delta_h}{\lambda_h} \quad (3)$$

The heat flux density can be computed from (4):

$$q = -(\lambda / \delta)\Delta T_{12} \quad (4)$$

On the basis of the operating principle (4), the conductive heat flux density from the heat source to the heat sink can be measured using the flat-plate heat-flux sensor.

A. Sensor Configurations

In order to decrease thermal resistance of the sensor to heat transfer, we choose materials with thermal conductivity relation $\lambda_h >> \lambda_l$ and thickness relation $\delta_h \approx \delta_l = \delta$. Figure 1 illustrates a basic configuration, where red copper with $\lambda_h = 390\text{W/(mK)}$ is chosen for the high conductivity material; and nylon with $\lambda_l = 0.53\text{W/(mK)}$ for the low conductivity material to create a measurable temperature difference. To illustrate the effect of the design parameters on the temperature difference and sensor linearity, two other alternatives (Figs. 2a and 2b) are designed:

- Improved design I (Fig. 2b): The nylon cylinder is modified to reduce its contact area with the red copper thereby partially eliminating the effect of the lateral heat flow around the common boundaries; heat flux q and common surface temperature T_c.
- Design configuration II (Fig.2b): A 2nd low conductivity material (nylon step cylinders) with a thin-film temperature sensor (RTD3) is added to obtain the 3rd temperature signal T_3. As in (3), $\Delta T_{13} = T_1 - T_3$ can be obtained similarly:

$$\Delta T_{13} = \Delta T_{12} = -q\delta / \lambda \quad \text{or} \quad q = -(\lambda / 2)\delta\Delta T_{12}$$

This implies that an equivalent thermal conductivity of λ/2 can be obtained. In addition, the dual ΔT provides a means to compensate measurement errors to some extent through sensor data fusion, and eliminate any possible incidental error of a single measurement.

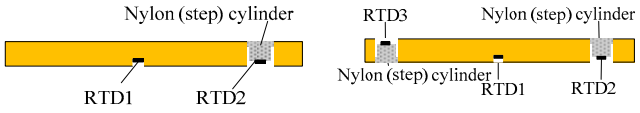

(a) Improved design I (b) Design configuration II

Fig. 2. Improved sensor configurations

The design configurations were experimentally tested with 7 different heating power levels:

0.2W, 0.48W, 1.8W, 3.2W, 5W, 7.2W and 9.8W

The results compared against the basic sensor configuration (Fig. 1) are given Figs. 3 and 4. Figure 3 compares the temperature differences of the basic design configuration and the improved design I. Temperature differences obtained using Design Configuration II are graphed in Fig. 4.

Some observations comparing the measurements of three designs are made as follows:

a) As shown in Fig. 3, improved design I exhibits more consistent and more responsive ΔT_{12} readings than the basic configuration, and also nearly doubles the ΔT_{12} values for the same heating power. The reduction of contact area from the λ_h plate to the λ_l cylinder, which eliminates the lateral heat transfer mostly, has a direct effect of increasing the

range and sensitivity of the temperature-difference measurement.

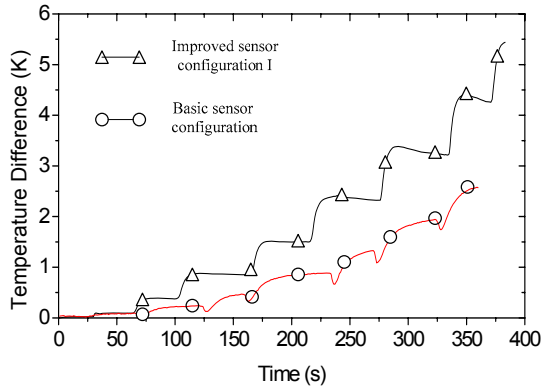

Fig. 3. Temperature difference of basic design and improved design I

b) Design Configuration II provides two possible readings (ΔT_{12}, ΔT_{13} and ΔT_{12}+ΔT_{13}). As shown in Fig. 4, ΔT_{12}+ΔT_{13} doubles the ΔT_{12} value as expected. In (4), the thermal conductivity λ is inversely proportional to ΔT for a given heat flux density. This implies that for a given low conductivity λ_l, an effective method to achieve high-resolution heat-flux measurement to use redundant sensor readings:

$$q = -(\lambda/\delta)\sum_{i=1}^{n_s}\Delta T_{1(i+1)} \approx -(\lambda/n_s)\delta\Delta T_{12}$$

where n_s is the number of ΔT readings.

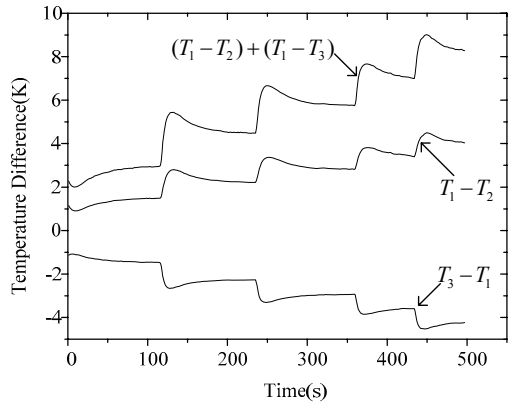

Fig. 4. Temperature difference of improved configuration II

B. Microcomputer-based Measurement Circuit

Figure 5 shows the schematic diagram of electronics, which consists a low constant current source, a microcomputer unit (MCU, SSTE564RD), and three thin-film Platinum resistance Pt1000 elements to be denoted in Fig. 5 as RTD1, RTD2 and RTD3 for temperature measurements each complete with a 24-bit analog-to-digital converter (ADC, AD7713).

To reliably convert the measured resistance R of the RTD into a voltage signal, a four-wire connection scheme is adopted to eliminate the lead resistance errors [11], and a μA-level constant current source is used to avoid the influence of the self-heating effect on the measurement accuracy [12], [13]. Signal noise is filtered digitally using the method of moving average:

$$y[n] = y[n-1] + (x[n] - x[n-N])/N \quad (5)$$

where $x[n]$ and $y[n]$ denote the input signal and the output signal respectively, n is the sampling order number of the measurement signal, and N is the latest sample numbers of the data sequence,

$$y[N-1] = (1/N)\sum_{i=1}^{N-1} x[N-i].$$

In (5), the division is implemented using shift operations; in this case, the filter only needs adders.

The temperature T can be calculated from the resistance-temperature characteristic equation (6):

$$R/R_0 = 1 + \alpha(T-273.15) + \beta(T-273.15)^2 \quad (6)$$

where R_0 is the resistance value of RTD at 273.15K (0°C); and α and β are constants in IEC751 standard. For a given R/R_0, the temperature value is given by (7):

$$T = 273.15 + (-\alpha + \sqrt{\alpha^2 - 4\beta(1-R/R_0)})/(2\beta) \quad (7)$$

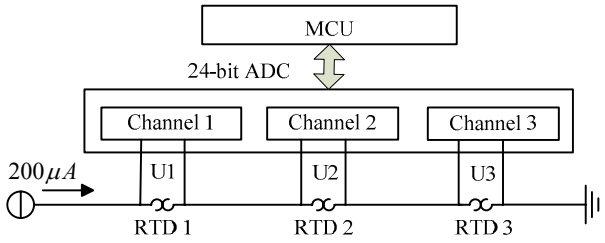

Fig. 5. Temperature data acqusition schematic diagram

Once the temperatures are known, the temperature differences (ΔT_{12}, ΔT_{13} and ΔT_{12}+ΔT_{13}) can be calculated. To provide the flexibility to account for the thermal inertia and accommodate a specific application characteristics, we define a threshold value ε based on the rate of change in ΔT_{12} and ΔT_{13} (denoted as $\Delta^2 T_{12}$ and $\Delta^2 T_{13}$ respectively). For example, if an object has large thermal inertia, the threshold value will be higher; otherwise, the threshold value will be lower. Assume that $\Delta^2 T_1$ and $\Delta^2 T_2$ are never greater than a given positive value ε at the same time. The temperature difference value (for Design Configuration II) can be obtained by the following piecewise function expression:

$$\Delta T = \begin{cases} 2\Delta T_{12}, & |\Delta^2 T_{13}| > \varepsilon \\ 2\Delta T_{13}, & |\Delta^2 T_{12}| > \varepsilon \\ \Delta T_{12} + \Delta T_{13}, & |\Delta^2 T_{12}| \le \varepsilon \text{ and } |\Delta^2 T_{13}| \le \varepsilon \end{cases} \quad (8)$$

To allow for calibration against modeling errors, the

corresponding heat flux density for a measured ΔT given by (8) can be calculated according to (9):

$$q = -k_m(\lambda_{eq}/\delta)\cdot\Delta T \tag{9}$$

where λ_{eq} is the equivalent thermal conductivity for ΔT, and k_m is a correction factor to be obtained from experimental calibration.

Figure 6 shows the flowchart summarizing the algorithmic steps executed by the embedded MCU of the heat-flux sensor. As shown in Fig. 6 the algorithm includes four parts; filtering (5), temperature calculation (7), temperature-difference calculation (8) and heat flux density calculation (9). The plate temperature is given by (10):

$$T_c = T_2 - q\delta_l/\lambda_l \tag{10}$$

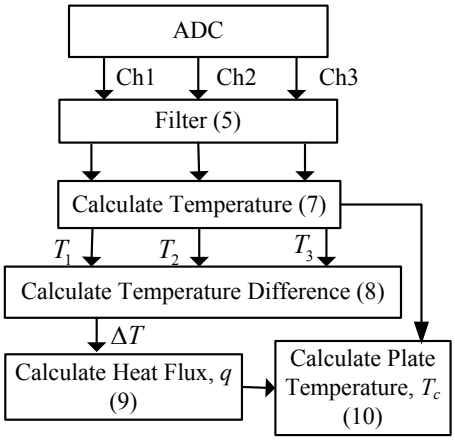

Fig. 6. Data processing algorithm flow diagram

III. Experimental Validation

A. Test Bed and Procedures

To demonstrate the concept feasibility of the heat-flux sensor and validate the algorithm system, the flat-plate heat-flux sensor has been fabricated and evaluated experimentally using the conductive test bed as shown in Fig. 7(a), which consists of the master test equipment, and other peripheral test devices (such as data acquisition instrument, adjustable DC power supply and computer recording). Figures 7(b) and 7(c) show respectively the assembled and exploded view of the master test equipment. As shown in Fig. (7b), the heat source is an electrical heating film controlled by the adjustable DC power supply. Insulation is placed around the heating element such that the heat flux flow (without leakage) from the heat source through the heat-flux sensor to a heat sink composed of a high conductivity metal block with fins, and a DC driver fan.

Specific parameters and design values characterizing the heat-flux sensor are given in Table II. The measured heat-flux computed following the steps outlined in Fig, 6 is given in Fig. 8. As a basis for validation, the measurements are compared against the theoretical heat flux density calculated by $q_t = Q/S$, where Q is the heating power of heating thin film; and S is the plate area of heat flux sensor.

Some discrepancies observed in Fig. 8 may be due to the following causes:

1) The insulation container does not completely prevent the heat leakage and hence, the sensor measures lower heat flux density than the theoretical value.
2) The lateral heat flow between copper plate and nylon cylinder cannot be eliminated completely.

The experiment data suggest that the sensitivity of the heat flux sensor can reach the level of 0.001-0.01K/ (W/m^2).

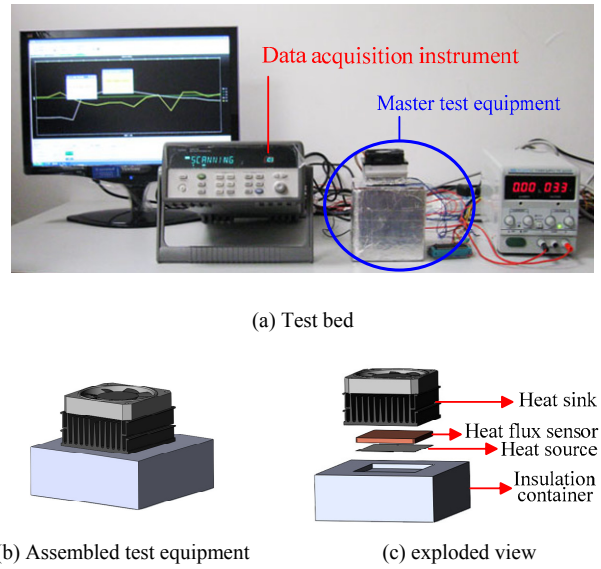

(a) Test bed

(b) Assembled test equipment

(c) exploded view

Fig. 7. Testbed for evaluation of the flat-plate heat-flux sensor

TABLE II
FABRICATION PARAMETER OF FLAT PLATE HEAT FLUX SENSOR

Parts coefficient	Thickness (mm)	Area (mm^2)	Conductivity (W/m^2)
Plate	3	1600	
Red Copper	3	1543.46	390
Nylon boss	2	56.54	0.53
RTD/Filter	α=3.9080 2×10^{-3}	β=-5.802$\times$ 10^{-7}	N=5
Calibrated parameters	k_m=1.2	λ_{eq}=0.265	

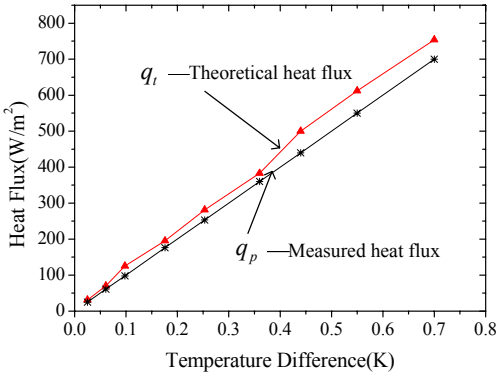

Fig. 8. Validation result of heat flux sensor

IV. Illustrative Application

Thermal management is an important topic in the design of the spacecraft such as the satellite and the spaceship. An essential procedure to verify its overall function is to perform a ground-based simulation of space radiation environment. Figure 9 shows an application where the flat-plate heat-flux sensor is employed as an equivalent physical simulator (EPS) for a nano-satellite [3]. The EPS constitutes a heat sink, one thermal electric cooler (TEC), and the flat-plate heat-flux sensor. TEC as an active actuator can control heat transfer under the control of a pulse width modulated (PWM) signal. The heat sink is responsible for dissipating the heat emitted by TEC. For the simulator test, the simulator is setup on the heat dissipation surface of nano-satellite as shown in Fig, 9.

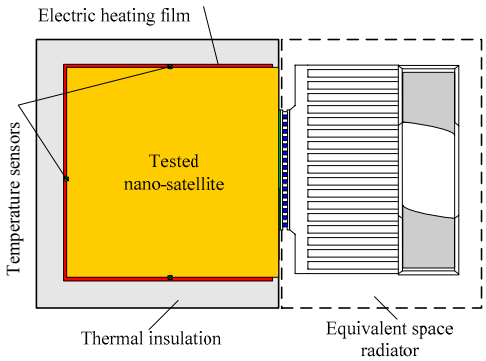

(a) EPS

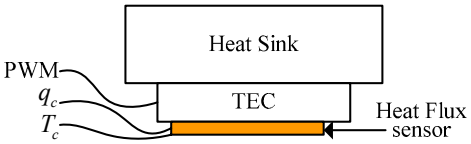

(b) Heat-flux sensor

Fig. 9. Schematics illsutarting EPS for a Nano-satellite

The basic principle of the EPS is to simulate the heat radiation using conductive heat transfer. In other words, the simulator is to track the radiation heat flux density with the conductive heat flux (Fig. 10), and it is given by

$$q_r = \varepsilon \sigma T_s^4 \tag{11}$$

where q_r is radiation heat flux; ε is surface emissivity of nano-satellite; σ is Stefan-Boltzmann constant; and T_s is the surface temperature of nano-satellite. Because the flat plate heat flux sensor I sin contact with the heat dissipation surface of nano-satellite, the satellite's surface temperature T_s is essentially the plate temperature T_c of the heat flux sensor. The conductive heat flux density q_c can be measured by the flat-plate heat-flux sensor.

As shown in Fig. 10, when the heat dissipation surface temperature of nano-satellite changes, the radiation heat flux density q_r varies according to (11). Based on the error e (between the radiative heat flux q_r and the conductive heat flux q_c), the PID controller manipulates the TEC adaptively through the PWM signals such that the conductive heat flux density q_c can track radiative heat flux density q_r. When temperature T_c changes, the heat flux tracking condition can be described as shown in Fig. 11. The results (Fig. 11) show that the conduction heat flux density track the radiation heat flux density closely with a small phase difference.

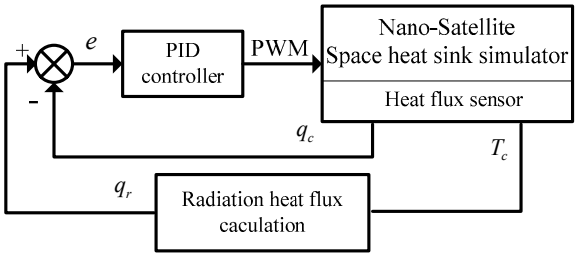

Fig. 10. Control diagram of simulator

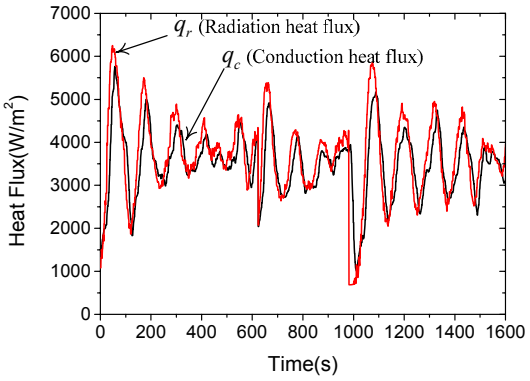

Fig. 11. Heat flux tracking of simulator

V. Conclusion

This paper presents the operating principle and design of a new flat-plate heat-flux sensor for conductive heat flux measurement based on temperature measurement with high accuracy has been presented. The sensor, which takes advantages of a pair of high and low thermal conductivities, can measure the temperature difference across the flat plate and the heat flux flowing through.

Aiming at eliminating the measurement error caused by effect of lateral heat flow, two improved sensor configurations have been carried out, and sensor configuration II added a temperature-difference measurement channel with one nylon step cylinder and one temperature sensor element, which provide a basis to improve the heat-flux resolution. Based upon the optimized sensor configuration II, a microcomputer controlled flat-plate heat-flux sensor has been developed, and test results show that the sensitivity of the heat flux sensor can reach the level of 0.001-0.01K/(W/m^2). To reveal research context and validate measurement performance of the plat-plate heat-flux sensor, an illustrative application where the sensor is

employed as an equivalent physical simulator (EPS) for a nano-satellite has been demonstrated and the experiment result show that the measurement value of the heat flux sensor can track reference heat flux value well.

Although a lot of design and validation work has been done in this paper, this research is still ongoing effort and further experiment must be made to analyze dynamic performance of the sensor and it is expected that this type of flat-plate heat flux sensor can be applied in other thermal management system, which needs conductive heat flux measurement.

REFERENCES

[1] J.W. Wan *et al*., "An Analysis of Two-Heater Active Thermal Control Technology for Device Class testing," *IEEE Trans. Components and Packaging Technologies*, vol. 27, pp. 577 – 584, Sept. 2004.

[2] Pu Liu, Hang Li, Lingling Jin, Wei Wu, S.X.-D Tan, and Jun Yang, "Fast Thermal Simulation for Runtime Temperature Tracking and Management," *IEEE Trans. Computer-Aided Design of Integrated Circuits and Systems*, vol. 25, pp. 2882– 2893, Dec. 2006.

[3] Yun-ze Li, Kok-meng Lee, Jun Wang, "Analysis and Control of equivalent Physical Simulator for Nanosatellite Space Radiator," *IEEE/ASME Trans. Mechatronics*. [online], available: http:// www.ieeexplore.com.

[4] R. Osiander, S.L. Firebaugh, J.L. Champion, D. Farrar, and M.A.G. Darrin, "Microelectromechanical Devices for satellite thermal control," *IEEE J. Sensors*, vol. 4, pp. 525 – 531, Aug. 2004.

[5] M. Karimifar , S. Aghanajafi, and A.B. Shabani, "Radiative Heat Flux Control Over Spherical Surfaces," in *Proc. 1997 IEEE Int. Conf. Intelligent Engineering Systems*, pp. 549 – 552.

[6] Jaechul Chun, S. Hwan Oh, Seung S. Lee, and Moohwan Kim, "Design and Fabrication of Micro Heat Flux Sensor," in *Proc. 1999 IEEE Int. Conf. Intelligent robots and system*, pp. 1045–1048.

[7] Lisa C. Martin, John D. Wrbanek, and Gustave C. Fralick, "Thin Film Sensor for Surface measurement," in *Proc. 1998 IEEE Int. Conf. thermoelecrics*, pp. 214-217.

[8] Vital. Meyer, Niklaus Schneeberger and Bruno Keller, "Epoxy-Protected Thermopile as High Sensitive Heat Flux Sensor," in *Proc. 1997 IEEE Int. Conf. Solid-state Sensors and Actuators*, pp. 1267-1270.

[9] Fricdcmann Volklein, and Ernst Kcsslcr, "Thermoelectric Microsensor for heat Flux Measurement," in *Proc. 1998 IEEE Int. Conf. thermoelectric*, pp. 214–217.

[10] Roman V. Lobach, Oleg V. Lobach, and Regina P. Dikareva, "The Case Development of a Heat Flux Sensor," in *Proc. 8th Int. Conf. siberian workshop and tutorials EDM*, pp. 113-114.

[11] Sorin-Dan Grigorescu, Constantin Iliescu and Brandusa Pantelmon, "A Sensor Self-heating Method for Lead's Resistance Compensation in Two Wires RTD's Measurements," in *Proc. 1994 Int. Conf. Precision electromagnetic measurement conference*, pp. 174-175.

[12] Eugeny A. Merkurjev, Sofia V. Voronova, Oleg V. Lobach and Roman V. Lobach, "Automation of Measurements of Parameters of the Heat Flux Sensor," in *Proc. 7th Int. Conf. siberian workshop and tutorials EDM*, pp. 305-308.

[13] V.F. Mitin, V.V. Kholevchuk and R.V. Konakova, "Temperature Microsensors", in *Proc. 1999 IEEE Int. Conf. Semiconductor*, pp. 495-498.